



This item was submitted to Loughborough's Institutional Repository (<https://dspace.lboro.ac.uk/>) by the author and is made available under the following Creative Commons Licence conditions.



CC creative commons  
COMMONS DEED

**Attribution-NonCommercial-NoDerivs 2.5**

**You are free:**

- to copy, distribute, display, and perform the work

**Under the following conditions:**

 **Attribution.** You must attribute the work in the manner specified by the author or licensor.

 **Noncommercial.** You may not use this work for commercial purposes.

 **No Derivative Works.** You may not alter, transform, or build upon this work.

- For any reuse or distribution, you must make clear to others the license terms of this work.
- Any of these conditions can be waived if you get permission from the copyright holder.

**Your fair use and other rights are in no way affected by the above.**

This is a human-readable summary of the [Legal Code \(the full license\)](#).

[Disclaimer](#) 

For the full text of this licence, please go to:  
<https://creativecommons.org/licenses/by-nc-nd/2.5/>

Elsevier Editorial System(tm) for International Journal of Fatigue  
Manuscript Draft

Manuscript Number:

Title: Unified methodology for the prediction of the fatigue behaviour of adhesively bonded joints.

Article Type: Research Paper

Section/Category:

Keywords: Damage mechanics; fatigue; strength degradation; backface strain; adhesive joint.

Corresponding Author: Dr Ian Anthony Ashcroft,

Corresponding Author's Institution:

First Author: Vikram Shenoy

Order of Authors: Vikram Shenoy; Ian A Ashcroft; Gary W Critchlow; Andrew D Crocombe

Manuscript Region of Origin: Europe

1  
2  
3 Unified methodology for the prediction of the fatigue behaviour of  
4 adhesively bonded joints.  
5  
6

---

7 V. Shenoy <sup>a</sup>, I. A. Ashcroft <sup>a</sup>, G. W. Critchlow <sup>b</sup>,  
8 A. D. Crocombe <sup>c</sup>.  
9

10  
11 <sup>a</sup> *Wolfson School of Mechanical and Manufacturing Engineering,*  
12 *Loughborough University, LE11, 3TU, UK.*

13  
14 <sup>b</sup> *Department of Materials,*  
15 *Loughborough University, LE11, 3TU, UK.*

16  
17 <sup>c</sup> *Faculty of Engineering and Physical Sciences, University of Surrey,*  
18 *Guildford, Surrey, GU2 5XH, UK.*  
19  
20  
21

22  
23  
24 **Abstract**  
25

26  
27  
28 A unified model is proposed to predict the fatigue behaviour of adhesively bonded joints. The model is  
29 based on a damage mechanics approach, wherein the evolution of fatigue damage in the adhesive is  
30 defined as a power law function of the micro-plastic strain. The model is implemented as an external  
31 subroutine for commercial finite element analysis software. Three dimensional damage evolution and  
32 crack propagation were simulated using this method and an element deletion technique was employed to  
33 represent crack propagation. The model was able to predict the damage evolution, crack initiation and  
34 propagation lives, strength and stiffness degradation and the backface strain during fatigue loading. Hence  
35 the model is able to unify previous approaches based on total life, strength or stiffness wearout, backface  
36 strain monitoring and crack initiation and propagation modelling. A comparison was made with  
37 experimental results for an epoxy bonded aluminium single lap joint and a good match was found.  
38  
39  
40  
41  
42  
43  
44  
45  
46  
47  
48

49  
50  
51 **Keywords:** Damage mechanics, fatigue, strength degradation, backface strain, adhesive joint.  
52  
53  
54  
55  
56  
57  
58  
59  
60  
61  
62  
63  
64  
65

# 1. Introduction

Bonded joints are increasing replacing conventional joints in structural applications, notably in the Aerospace, Automotive and Marine industries. This is mainly due to mechanistic advantages such as; high strength and stiffness to weight ratio and reduced stress concentrations, however, cost savings can also be made. This has lead to challenges in the field of designing such joints, especially under fatigue loading, which is the typical loading type in most structural applications. Lifetime prediction under fatigue loading is an important part of the design process and can be used to optimise the joint design and inform in-service monitoring procedures as well as indicating the safe life of the joint under various conditions. Many methods of predicting and characterising fatigue life in bonded joints have been proposed [1]; however, to date the various approaches have been limited in their functionality and applicability.

The methods of predicting fatigue lifetime can generally be classified as; total-life, Palmgren-Miner (PM) based, phenomenological based and progressive damage models. Several reviews have been published [2-3] regarding usage of these models for metals and for composite materials and more recently for bonded joints [1]. It can be concluded from these reviews that while total life based approaches are the simplest to apply; they have limited scope in the lifetime prediction of bonded joints, especially in the case of variable amplitude fatigue.

PM based models, as first proposed by Palmgren [4] and Miner [5], are also simple to apply and are used to predict fatigue lifetime under variable amplitude fatigue loading through the assumption of linear damage accumulation. However, they are generally not able to account for load interaction and load sequencing effects present in a variable amplitude fatigue loading spectrum. In addition, none of the approaches discussed so far (both total life and PM rule based) can be used to monitor the damage in the sample as only the final failure is characterised. This can be achieved through the application of phenomenological models.

1  
2  
3 Phenomenological models represent change in the strength or stiffness under fatigue loading and can  
4  
5 incorporate factors to model variable amplitude fatigue. However, these models are highly dependent on  
6  
7 joint specific experimental results and in the case of strength wearout require destructive experimental  
8  
9 testing. Recent work has demonstrated the effectiveness of the strength wearout approach to predict  
10  
11 fatigue lifetime under both constant and variable amplitude fatigue loadings [6-9]. However, a more  
12  
13 flexible and direct method of representing fatigue degradation is through progressive damage modelling.  
14  
15

16  
17 Progressive damage models can be either fracture mechanics (FM) or damage mechanics (DM) based. In  
18  
19 the case of FM based models, the crack propagation phase is assumed to be dominant and is characterised  
20  
21 by an empirical crack growth law. The most extensively used crack growth laws are based on the one  
22  
23 proposed by Paris and Erdogan [10]. In this model the crack growth rate is defined as a power law  
24  
25 function of stress intensity factor in the crack tip region. In the case of bonded joints, strain energy  
26  
27 release rate is usually used instead of stress intensity factor [11-15]. A FM based approach has also been  
28  
29 proposed for variable amplitude fatigue where a damage shift factor was used to account for load  
30  
31 interaction effects [16]. However, the main draw-back to the FM approach is that it does not account for  
32  
33 crack initiation prior to macro-crack growth. For example, when bonded single lap joints (SLJ) are  
34  
35 considered, the crack initiation was found to dominate the fatigue life at high cycles [17], and in such  
36  
37 cases the Paris law method of lifetime prediction will under predict the fatigue lifetime.  
38  
39  
40

41  
42 Using a DM based approach, the evolution of damage prior to macro-crack growth can be simulated. In  
43  
44 these models the main requirement is to define a damage variable to represent the severity of material  
45  
46 damage during fatigue loading. In the case of composite materials, models have been proposed to  
47  
48 simulate delamination and damage in the matrix [18, 19]. These models can be characterised based on the  
49  
50 type of damage growth law and the parameters used to define them, which include matrix crack density in  
51  
52 the case of glass fibre reinforced plastic composites [19] and a thermodynamic potential based strain  
53  
54 energy density in the case of carbon fibre composites [18]. To date, little on the application of DM to the  
55  
56 fatigue life of bonded joints can be found in the literature, however Abdel Wahab et al. [20] used a  
57  
58  
59  
60  
61  
62  
63  
64  
65

1  
2  
3 continuum damage mechanics (CDM) approach to predict the fatigue lifetime of bonded double lap joints  
4  
5 and found this compared favourably with the FM based approach. However, no attempt was made to  
6  
7 incorporate the CDM approach in a progressive damage model.  
8  
9

10 It can be seen that, all of the models discussed can be useful in characterising or predicting fatigue  
11  
12 behaviour under certain conditions but that all have limited applicability and functionality, and it appears  
13  
14 that no attempt has yet been made to propose a methodology that is widely applicable and can be used to  
15  
16 generate all the data from the methods discussed. In this paper a unified fatigue methodology (UFM) is  
17  
18 proposed, wherein a single damage evolution law is used to predict all the main parameters characterising  
19  
20 the fatigue life of bonded joints. These consist of progressive damage evolution, crack initiation and  
21  
22 propagation lives, backface strain (BFS) characterisation and strength and stiffness wearout. In this way a  
23  
24 single damage evolution law is used to unify all previous approaches to characterising and predicting  
25  
26 fatigue in bonded joints.  
27  
28  
29  
30  
31

## 32 2. Unified fatigue methodology (UFM) 33

34 In this methodology a damage evolution law is used to predict the main parameters governing fatigue life.  
35  
36 The model is described in Fig. 1. The inputs for the method are; material properties, joint geometry and  
37  
38 boundary conditions. A small number of fatigue-life test results are required to determine the constants in  
39  
40 the damage evolution law. Various algorithms are used to determine the different outputs as described in  
41  
42 the following subsections.  
43  
44  
45

### 46 2.1 Progressive damage modelling 47

48  
49  
50 The rate of damage evolution was assumed to be a power law function of the equivalent micro plastic  
51  
52 strain, i.e.:

$$53 \frac{dD}{dN} = m_1 (\epsilon_p)^{m_2} \quad (1)$$

54  
55  
56  
57  
58  
59  
60  
61  
62  
63  
64  
65

1  
2  
3 where,  $D$  is the damage variable, which is equal to 0 for undamaged material and 1 for completely  
4  
5 damaged material.  $N$  is the number of fatigue cycles and hence  $dD/dN$  is the damage rate.  $m_1$  and  $m_2$  are  
6  
7 experimentally determined constants and  $\epsilon_p$  is the localised equivalent plastic strain. Plastic strain was  
8  
9 used as the parameter for damage progression in this approach as this is a convenient method of  
10  
11 introducing a level of strain below which, damage does not occur. Also, the region of high equivalent  
12  
13 plastic strain matches well with the region of damage observed optically in sectioned and polished  
14  
15 samples, as shown in Fig. 2. Note that the adherend is not shown in Fig. 2(b) to aid clarity and only half  
16  
17 the sample width is shown owing to the use of symmetry in the model. Hence, the area of maximum  
18  
19 equivalent plastic strain indicated in the figure is in the middle of the sample width. The damage model  
20  
21 can be implemented in commercial finite element software via an external subroutine. Eqn. 1 can be  
22  
23 numerically integrated over each element in the model to simulate damage evolution followed by crack  
24  
25 propagation for fully damaged elements (i.e. where  $D = 1$ ). Using this algorithm, the number of cycles to  
26  
27 failure for different fatigue loads can be calculated. The constants  $m_1$  and  $m_2$  can be optimised based on  
28  
29 fatigue life data for two or three different loads spanning the range to be considered.  
30  
31

## 32 33 34 35 2.2 Prediction of damage evolution and crack initiation and propagation 36

37  
38 The immediate results of the model described in the last section are 3D maps of damage evolution and  
39  
40 crack propagation as a function of cycles for different fatigue loads. This data is conveniently represented  
41  
42 as plots of damage and crack length vs. number of fatigue cycles. In terms of damage, this can be viewed  
43  
44 for individual elements or averaged over an area of interest. This information can be used to determine the  
45  
46 location and extent of damage in the adhesive layer at any time in the fatigue life. The fatigue initiation  
47  
48 life is defined as the number of cycles prior to complete damage of an element or the number of cycles to  
49  
50 generate a crack of predetermined size. Once a crack has initiated, the damage in elements ahead of the  
51  
52 crack can be used to study the size and shape of the process zone. Any overloads in the fatigue spectrum  
53  
54 will increase damage in the elements ahead of the crack. Hence, the crack acceleration which has been  
55  
56  
57  
58  
59  
60  
61  
62  
63  
64  
65

1  
2  
3 observed in the variable amplitude fatigue testing of bonded joints [7, 9, 21] can potentially be modeled  
4  
5 using this approach, without the need for any further empirical interaction factors, as in [9, 16]. It is also  
6  
7 interesting to note that if a visco-elastic/ plastic constitutive model was used for the adhesive, then time  
8  
9 dependent straining would occur under load that would increase damage. This, potentially, could be used  
10  
11 to model the creep enhanced fatigue failure of bonded joints reported in previous work [15, 22]. Hence,  
12  
13 UFM also has the potential to unify the methods used to characterise variable amplitude fatigue and creep  
14  
15 fatigue in adhesively bonded joints. Once a macro-crack has formed, the size and shape of the crack as a  
16  
17 function of cycles is generated, as in the FM based methods.  
18  
19  
20

### 21 2.3 Extended L-N curve prediction 22 23 24

25 Load-life (L-N) is often plotted instead of stress-life for bonded joints. This is because stress in bonded  
26  
27 joints is extremely non-uniform and there is no simple relation between the easily measured average shear  
28  
29 stress in a lap joint and the maximum stress. Hence, it is sensible to use load in the place of stress to  
30  
31 define the fatigue life. The total fatigue life,  $N_f$ , can be divided into crack initiation and propagation lives  
32  
33 as:  
34  
35

$$36 \quad N_f = N_i + N_p \quad (2)$$

37  
38 where,  $N_i$  is the number of cycles to macro-crack initiation and  $N_p$  is the number of cycles associated with  
39  
40 crack propagation prior to complete failure. It is possible to predict both  $N_i$  and  $N_p$  in addition to  $N_f$ , from  
41  
42 the data described in the previous section. These can be plotted as a function of fatigue load, as shown  
43  
44 schematically in Fig. 3. The resultant plot shows the proportion of the fatigue life spent in crack initiation  
45  
46 and propagation, in addition to total fatigue life, and has been termed an extended L-N diagram.  
47  
48  
49  
50  
51

### 52 2.4 Strength and stiffness wearout and BFS prediction 53 54 55 56 57 58 59 60 61 62 63 64 65



1  
2  
3 A reduction in the strength or stiffness of bonded joints on fatigue loading is associated with an increase  
4  
5 in damage in the adhesive. As damage in the adhesive is simulated using eqn. (1), strength and stiffness  
6  
7 wearout can be expected. The decrease in strength of a joint owing to the modelled fatigue damage can be  
8  
9 calculated by applying an increasing load to the joint until it fails. This can be done using an algorithm  
10  
11 similar to the one described in section 2.1 for checking if  $N_f$  has been reached. Once the adhesive is  
12  
13 damaged or cracked, a series of increasing loads can be applied until the model becomes unstable for the  
14  
15 applied load. The instability in the model indicates that the joint cannot bear the applied load and thus an  
16  
17 approximate value of the failure load (or residual strength) can be deduced. This method was found to  
18  
19 work well in this case, however, alternative quasi-state failure criteria may also be used in a similar  
20  
21 fashion.  
22  
23  
24

25 In the case of stiffness wearout, at each damage increment in the model, the displacement at the loaded  
26  
27 end of the joint for the applied maximum fatigue load can be calculated. Using this displacement and the  
28  
29 applied load, the stiffness of the joint can easily be calculated. BFS can be calculated by measuring strain  
30  
31 under load at any location in the joint in the same algorithm. For every increment in the damage, the  
32  
33 average elastic strain on the back-faces of the adherend at any desired location can be calculated. This  
34  
35 stage can be extended to include practically any other useful means of characterising fatigue damage,  
36  
37 such as internal stresses and strains or natural modes and frequencies of vibration.  
38  
39  
40  
41

### 42 3. Implementation and experimental validation of the unified fatigue methodology 43 44 (UFM) 45

46 The UFM was implemented using an external subroutine written in Python script language for the MSC  
47  
48 Marc finite element analysis (FEA) software. The model was implemented for bonded SLJs manufactured  
49  
50 according to British standards BS ISO (4587:2003). The adherends were 7075 T6 aluminium alloy and  
51  
52 the adhesive used was Cytec FM 73M. The joint geometry is shown in Fig. 4. Fatigue testing was at 5 Hz  
53  
54 with a load ratio of 0.1. Further details of the experimental work can be found in [8, 17].  
55  
56  
57  
58  
59

### 3.1 Finite element details

The commercial FEA package MSC Marc was used for all the simulations. Eight noded hexahedral elements (Element 7 in MSC Marc) were used for the finite element mesh. Both material and geometric non-linearity were accounted for in the analysis. A typical mesh taken from a finite element model is shown in Fig. 5. The joint was constrained in the vertical direction at the loaded end of the joint, as shown in Fig. 6. In addition symmetric conditions (both planar and rotational) were applied enabling only a quarter of the joint to be modelled and thereby saving computation time.

Non-linear material properties were used in all the models. The Young's moduli for adhesive and aluminium alloy were 2GPa and 70GPa respectively. The Mohr-Coulomb model [23] was used for the adhesive and linear elasticity was assumed for the aluminium alloy as no plastic deformation was observed in the adherends during the experiments. For the Mohr-Coulomb model, a tensile yield stress equal to 28.73 MPa with yield surface modifier equal to 0.001057 was used (Jumbo, [24]). An isotropic hardening behaviour was assumed.

### 3.2 Progressive damage modelling

The model described in section 2.1 was implemented using an external subroutine written in Python © (Python Software Foundation Inc., Hampton, USA) script with the FEA software. The algorithm used for this purpose is shown in Fig. 7. This can be described in following steps.

Step 1: a finite element model is built and the values for number of cycles,  $N$ , and damage,  $D$ , are set to zero.

Step 2: a non-linear static analysis is carried out and plastic strain is determined for all the elements in the adhesive layer.

1  
2  
3 Step 3: check if the analysis converges, if yes then step 4, otherwise  $N = N_f$  and stop the program.  
4

5  
6 Step 4: the damage rate  $dD/dN$  is determined for each element in the adhesive using eqn. 1.  
7

8  
9 Step 5: the new value of damage in each element is calculated using the damage rate calculated in the  
10 previous step as:

$$D = D + \frac{dD}{dN} dN \quad (3)$$

16 where,  $dN$  is the increment to number of cycles.  
17  
18

19  
20 Step 6: check if  $D=1$ , if yes then delete the element, and go to step 2.  
21  
22

23 Step 7: if  $D \neq 1$  calculate new material properties as:  
24

$$E = E_0(1 - D) \quad (4)$$

$$\sigma_{yp} = \sigma_{yp0}(1 - D) \quad (5)$$

$$\beta = \beta_0(1 - D) \quad (6)$$

25  
26  
27  
28  
29  
30  
31  
32  
33  
34 where,  $E_0$ ,  $\sigma_{yp0}$  and  $\beta_0$  are Young's modulus, yield stress and plastic surface modifier constant for the  
35 parabolic Mohr-Coulomb model respectively.  
36  
37  
38

39  
40 Step 8: calculate new value of  $N$ ; go to step 2 and repeat.  
41  
42

43 The constants  $m_1$  and  $m_2$  were determined by repeating the procedure above for different values at two  
44 different fatigue loads and optimising. These constants were then kept constant to determine the life for  
45 other fatigue loads. In this way,  $m_1$  and  $m_2$  were used to completely characterise the fatigue damage and  
46 failure of the SLJs.  
47  
48  
49  
50  
51  
52  
53  
54  
55  
56  
57  
58  
59  
60  
61  
62  
63  
64  
65

### 3.3 Evolution of damage and crack propagation

The maximum equivalent plastic strain in the middle of the adhesive layer is plotted across the width of the SLJ in Fig. 8 (a), for a maximum fatigue load of 7.5kN and for zero cycles (i.e undamaged). This load was 63% of the quasi-static failure load (QSFL), which was 11.95 kN, with a standard deviation of 0.31 [8]. It can be seen that the maximum strain occurs in the middle of the joint width, which is at zero on the Z axis because of the symmetric boundary conditions applied during the analysis. The strain is constant in the central region but decreases rapidly at the sample edges. This is consistent with experimental observations that the first cracks always appear in the central region of the SLJ, in the fillet region [8]. In Fig. 8 (b) the plastic strain along the overlap length in the middle of the bondline is shown. It can be seen that the maximum strain is at the end of the overlap region, i.e. below the embedded adherend corner. This is in agreement with the location of first signs of damage and cracking in the joints [8, 17].

Damage progression in an element close to the embedded corner is plotted against number of cycles for different fatigue loads in Fig. 9(b). Similar behaviour was also found in other elements during the simulation. It can be seen that a non-linear increase in damage was found with an acceleration towards the onset of cracking (denoted by  $D=1$ ). When damage equals unity the element is deleted, hence creating a crack in the adhesive. The damage plot in Fig. 9(b) is for the element E shown in the finite element mesh in Fig. 9(a).

The crack growth (in the central section) for two different fatigue loads is plotted against number of cycles in Fig. 10. Elements were progressively deleted after the first crack formation and varied across the sample width. The crack lengths plotted in this figure are the crack lengths determined at the central section of the adhesive width, however the crack, also travels across the adhesive width during the simulation. This is in agreement with the experimental observations, wherein different lengths of cracks were found at different points across the adhesive. The predicted crack growth calculated is compared with experimental results in the same figure. It can be seen that there is a good match between predicted

1  
2  
3 and experimental results. The experimental details regarding the measurements of crack lengths can be  
4  
5 found in [8, 17].  
6

### 7 8 9 3.4 Extended S-N curve prediction

10  
11  
12 The total fatigue life calculated using the UFM matches well with the experimental results as shown in  
13  
14 Fig. 11 (a), where, the experimental results are taken from earlier work by the same authors [8, 17]. The  
15  
16 total life can be divided into initiation and propagation phases, as explained in section 2.3. It can be seen  
17  
18 in Fig. 11 (a) that the predicted proportion of initiation life increases as the fatigue load decreases, as also  
19  
20 seen in experiments [17]. The crack propagation life predicted using UFM is compared with that  
21  
22 predicted using a fracture mechanics (FM) approach in Fig. 11 (b). More details of the FM approach are  
23  
24 given in [20]. It can be seen that there is a difference in the gradient of the predicted propagation life, with  
25  
26 the UFM method showing less load dependency, however, the predicted number of cycles spent in  
27  
28 propagation to failure agree fairly well.  
29  
30  
31

### 32 33 3.5 Strength and stiffness wearout and BFS prediction

34  
35  
36  
37 In order to determine the strength degradation, a series of quasi-static loads were applied at each damage  
38  
39 increment until the finite element model became unstable. The highest load at which the model converged  
40  
41 was taken as an approximate value of the residual failure load of the joint. Stiffness degradation was  
42  
43 calculated by applying the maximum fatigue load to the joint and using the deflection of the joint under  
44  
45 load to calculate stiffness.  
46  
47  
48

49 In Fig. 12 strength wearout results are plotted against number of cycles for two different fatigue loads. It  
50  
51 can be seen that strength decreases non-linearly with respect to number of cycles with an accelerated  
52  
53 strength degradation towards the end of the fatigue life. The predicted values are compared with  
54  
55 experimental results taken from [8] in the figure. Excellent agreement between the predicted and  
56  
57  
58  
59  
60  
61  
62  
63  
64  
65

1  
2  
3 experimental results can be seen. The UFM was also used to predict the stiffness wearout of the SLJs by  
4 periodically determining joint displacement throughout the fatigue life. The predicted stiffness wearout is  
5 compared with experimental results for a maximum fatigue load of 7.5kN in Fig. 13. Similar to the  
6 strength wearout, it can be seen that the stiffness wearout is non-linear with an accelerated degradation  
7 towards the end of the fatigue life. There is a reasonable agreement between experimental and predicted  
8 strength wearout, however, the experimental results show a sharper decrease. This may be because of a  
9 lack of sensitivity in the experimental displacement measurements.  
10  
11  
12  
13  
14  
15  
16  
17  
18

19 An important method of monitoring fatigue degradation in adhesively bonded joints in-situ is through the  
20 measurement of BFS [17, 25-27]. Experimental values of BFS are compared with predicted values in Fig.  
21 14, where experimental values are taken from [17]. Similar values and trends can be seen in the  
22 experimental and predicted results. The difference in results can be attributed to the absence of an exact  
23 crack propagation scenario in the prediction. In the simulation, symmetric crack growth from both ends of  
24 the overlap was assumed, whereas asymmetric crack growth is often observed in practice. A more  
25 detailed explanation of these asymmetries is given in earlier work on BFS by the same authors [17].  
26  
27  
28  
29  
30  
31  
32  
33  
34

### 35 3.6 Summary

36  
37  
38  
39 In order to summarise the capabilities of the proposed UFM, the block diagram shown in Fig. 1 is  
40 redrawn in Fig. 15, with the results from the constant amplitude fatigue testing of an adhesively bonded  
41 SLJ. The hub of the method is the damage propagation law given in eqn. 1. The main input data are the  
42 material properties, joint geometry and boundary conditions. Two fatigue life data results were used to  
43 determine the constants in damage growth law for the particular joint. These were then used for all other  
44 fatigue loads.  
45  
46  
47  
48  
49  
50  
51  
52

53 Output consists of, firstly, damage evolution and crack propagation predictions as functions of the number  
54 of cycles and the fatigue load. Secondly, the extended L-N (or S-N) curve can be plotted, which shows  
55  
56  
57  
58  
59  
60  
61  
62  
63  
64  
65

1  
2  
3 both initiation and propagation lives as a function of fatigue load. Finally, damage monitoring parameters  
4 such as strength wearout, stiffness wearout and BFS can also be determined as functions of the number of  
5 fatigue cycles and the fatigue load. Hence, it has been shown that a single damage evolution law can be  
6 an effective tool in unifying the prediction of all the important characterisation of fatigue in bonded joints.  
7  
8  
9

## 10 11 12 13 14 6. Conclusions

15  
16 It has been shown that a damage progression law governed by equivalent plastic strain can be used as a  
17 unified method to predict all the major parameters associated with fatigue in bonded joints. Output from  
18 the method includes, BFS, strength and stiffness wearout, 3D damage evolution and crack propagation  
19 maps and fatigue initiation and propagation lives. The technique is versatile and potentially can be used to  
20 also predict variable amplitude fatigue and combined creep fatigue with little further adaptation.  
21  
22  
23  
24  
25  
26  
27

## 28 29 7. References

- 30  
31  
32  
33  
34 1. Ashcroft IA, Crocombe AD. Fatigue in adhesively bonded joints. In: da Silva, LFM, Oechsner,  
35 Andreas., Modelling failure in adhesively bonded joints. Springer, 2008; 184-187.  
36  
37  
38 2. Degrieck J, Van Paepegem W. Fatigue damage modelling of fibre reinforced composite  
39 materials. Applied mechanics review 2001; 54(4): 279-300.  
40  
41  
42 3. Fatemi A, Yang L. Cumulative fatigue damage and life prediction theories: a survey of the state  
43 of the art for homogeneous materials. International journal of fatigue 1998; 20: 9-34.  
44  
45  
46 4. Palmgren A. Die Lebensdauer von Kugellagen. des Vereins Deutscher Ingenieure 1924; 68: 339-  
47 341.  
48  
49  
50 5. Miner MA. Cumulative damage in fatigue. Journal of applied mechanics 1945; 67: A159-A 164.  
51  
52  
53 6. Schaff JR, Davidson BD. Lifetime prediction methodology for composite structures Part II -  
54 spectrum fatigue. Journal of composite materials 1997; 31: 158-181.  
55  
56  
57  
58  
59  
60  
61  
62  
63  
64  
65

- 1  
2  
3 7. Erpolat S, Ashcroft IA, Crocombe AD, Abdel-Wahab MM. A study of adhesively bonded joints  
4 subjected to constant and variable amplitude fatigue. *International journal of fatigue* 2004;  
5 26:1189-1196.  
6
- 7  
8 8. Shenoy V, Ashcroft IA, Critchlow GW, Crocombe AD, Abdel Wahab MM. Strength wearout of  
9 adhesively bonded joints under constant amplitude fatigue. *International journal of fatigue* 2009;  
10 [doi:10.1016/j.ijfatigue.2008.11.007](https://doi.org/10.1016/j.ijfatigue.2008.11.007).  
11
- 12  
13 9. Shenoy V, Ashcroft IA, Critchlow GW, Crocombe AD, Abdel Wahab MM. An evaluation of  
14 strength wearout models for the lifetime prediction of adhesive joints subjected to variable  
15 amplitude fatigue. *International journal of adhesion and adhesives* 2009; in press.  
16
- 17  
18 10. Paris P, Erdogan F. A critical analysis of crack propagation law. *Journal of basic engineering*,  
19 trans. ASME 1963: 528-534.  
20
- 21  
22 11. Ripling EJ, Mostovoy S, Patrick RL. Application of fracture mechanics to adhesive joints, in:  
23 Adhesion. ASTM STP 1963; 360.  
24
- 25  
26 12. Kinloch AJ, Osiyemi OS. Predicting the fatigue life of adhesively bonded joints. *Journal of*  
27 *adhesion* 1993; 43: 79-90.  
28
- 29  
30 13. Mall S, Johnson WS. Characterisation of mode I and mixed mode failure of adhesive bonds  
31 between composite adherends. NASA Technical Memorandum 86355, Hampton, NASA, 1985.  
32
- 33  
34 14. Erpolat S, Ashcroft IA, Crocombe AD, Abdel-Wahab MM. On the analytical determination of  
35 strain energy release rate in bonded DCB joints. *Engineering fracture mechanics* 2004; 71:1393-  
36 1401.  
37
- 38  
39 15. Al-Ghamdi AH, Ashcroft IA, Crocombe AD, Abdel Wahab MM. Crack growth in adhesively  
40 bonded joints subjected to variable frequency fatigue loading. *Journal of adhesion* 2003; 79:  
41 1161-1182.  
42
- 43  
44 16. Ashcroft IA. A simple model to predict crack growth in bonded joints and laminates under  
45 variable amplitude fatigue. *Journal of strain analysis* 2004; 39: 707-716.  
46
- 47  
48 17. Shenoy V, Ashcroft IA, Critchlow GW, Crocombe AD, Abdel Wahab MM. An investigation into  
49 crack initiation and propagation behaviour of bonded single-lap joints using backface strain.  
50 *International journal of adhesion and adhesives* 29 (2009) 361-371.  
51
- 52  
53 18. Daudeville L, Ladeveze P. A damage mechanics tool for laminate delamination. *Composite*  
54 *structures* 1993; 25: 547-555.  
55
- 56  
57 19. Ogin SL, Smith PA, Beaumont WR. Matrix cracking and stiffness reduction during the fatigue of  
58 a (0/90) s GFRP Laminate. *Composite science and technology* 1985; 22: 23-31.  
59  
60  
61  
62  
63  
64  
65



- 1  
2  
3 20. Abdel Wahab MM, Ashcroft IA, Crocombe AD, Shaw SJ. Prediction of fatigue threshold in  
4 adhesively bonded joints using damage mechanics and fracture mechanics. *Journal of adhesion*  
5 *science and technology* 2001; 7: 763-781.  
6  
7  
8 21. Erpolat S, Ashcroft IA, Crocombe AD, Abdel-Wahab MM. Fatigue crack growth acceleration  
9 due to intermittent overstressing in adhesively bonded CFRP joints. *Composites part A: applied*  
10 *science and manufacturing* 2004; 35: 1175-1183.  
11  
12  
13  
14 22. Al-Ghamdi AH, Ashcroft IA, Crocombe AD, Abdel Wahab MM. Creep and fatigue crack growth  
15 in DCB joints. In: *Proc 7<sup>th</sup> International conference on structural adhesives in engineering*, IOM  
16 *communications London*, 2003, pp. 22-25.  
17  
18  
19  
20 23. Coulomb CA. Essai sur une application des regles des maxims et minimus a quelques  
21 problemes de statique relatifs, a la architecture. *Mem. Acad.Roy. Sav* 1776; 7: 343-387.  
22  
23  
24 24. Jumbo SF. Modelling of residual stresses and environmental degradation in adhesively bonded  
25 joints, PhD thesis, Wolfson School of Mech and Manu Engg 2007; Loughborough University,  
26 Loughborough.  
27  
28  
29 25. Zhang Z, Shang JK, Lawrence FV. A backface strain technique for detecting fatigue crack  
30 initiation in adhesive joints. *Journal of adhesion* 1995; 49 (1-2): 23-36.  
31  
32  
33 26. Crocombe AD, Ong AD, Chan CY, Abdel-Wahab MM, Ashcroft IA. Investigating fatigue  
34 damage evolution in adhesively bonded structures using backface strain measurement. *Journal of*  
35 *adhesion* 2002; 78: 745-778.  
36  
37  
38 27. Graner-Solana A, Crocombe AD, Abdel-Wahab MM, Ashcroft IA. Fatigue initiation in  
39 adhesively bonded single lap joints. *Journal of adhesion science and technology* 2007; 21: 1343-  
40 1357.  
41  
42  
43  
44  
45  
46  
47  
48  
49  
50  
51  
52  
53  
54  
55  
56  
57  
58  
59  
60  
61  
62  
63  
64  
65

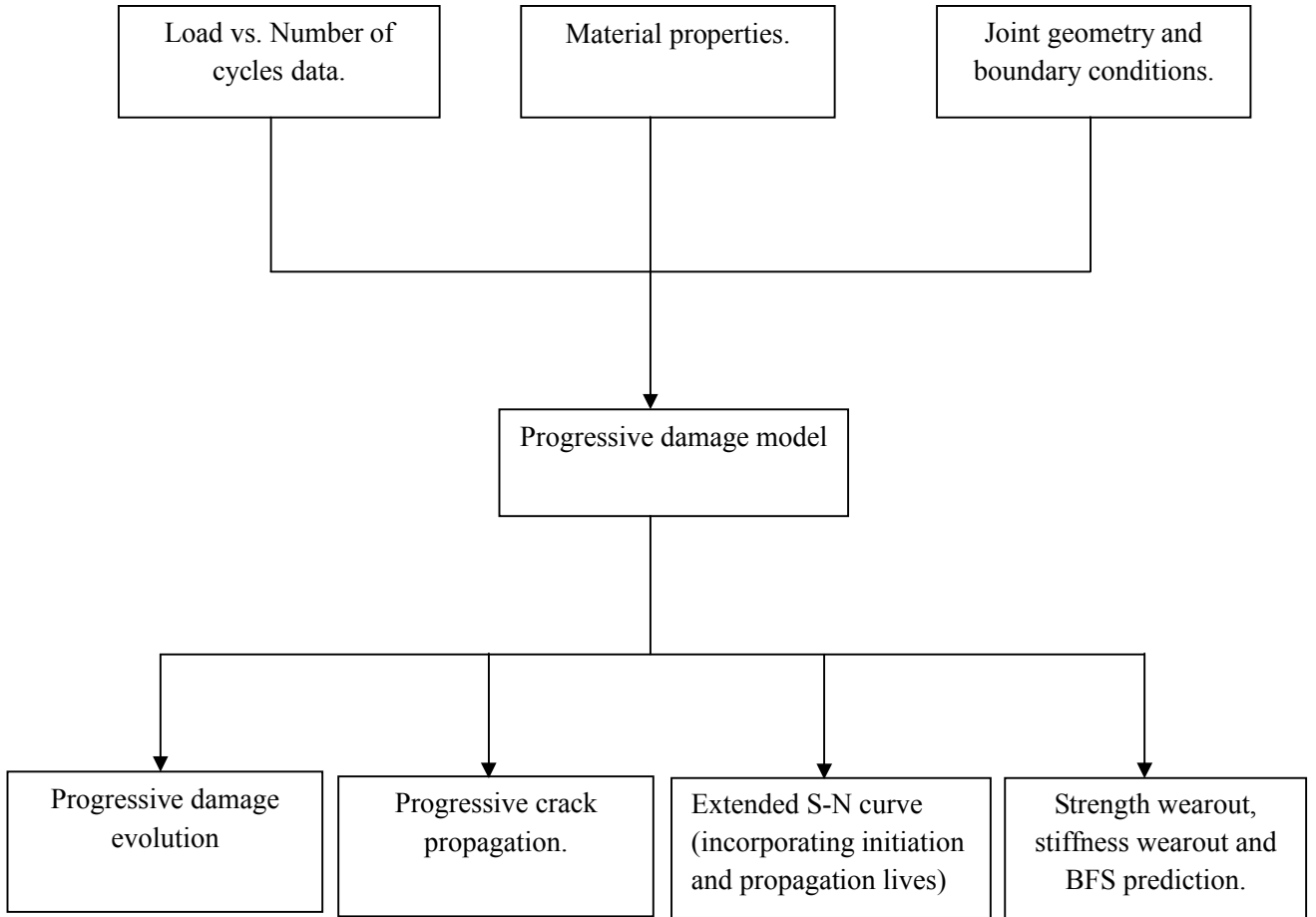


Fig. 1. Schematic representation of Unified Fatigue Methodology.

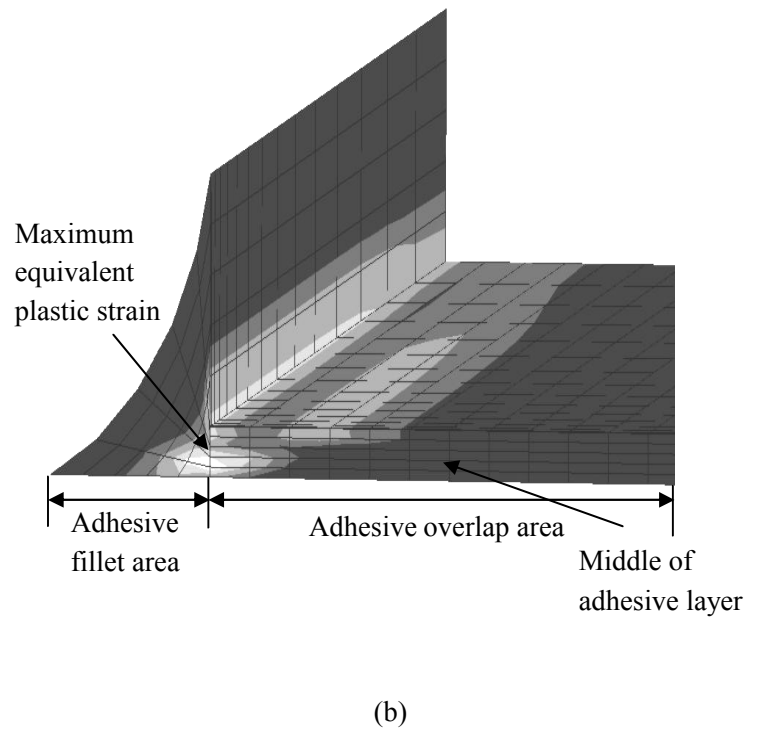
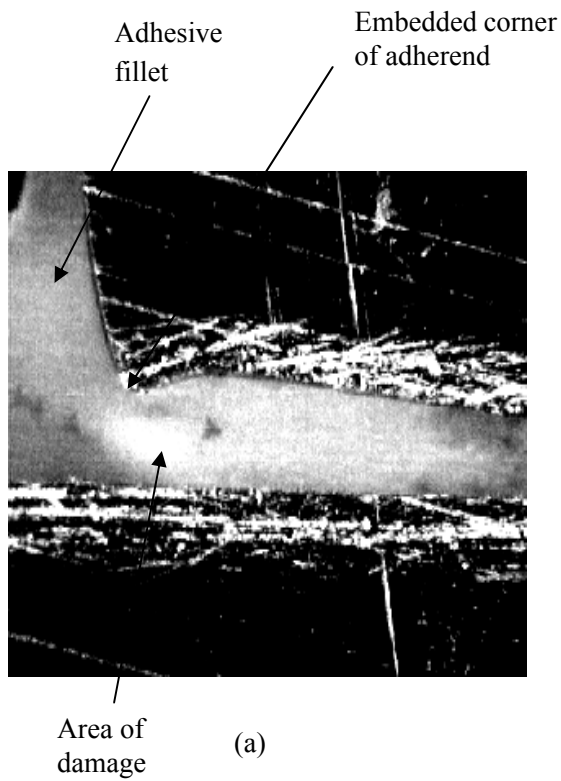


Fig. 2. Comparison between (a) damaged region observed in polished cross section and (b) the location of maximum equivalent plastic strain shown in finite element mesh of adhesive layer.

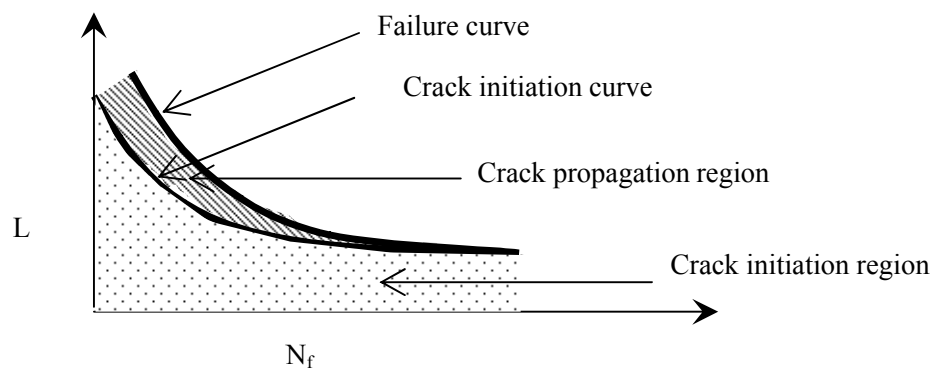


Fig. 3. Schematic representation of extended L-N diagram.

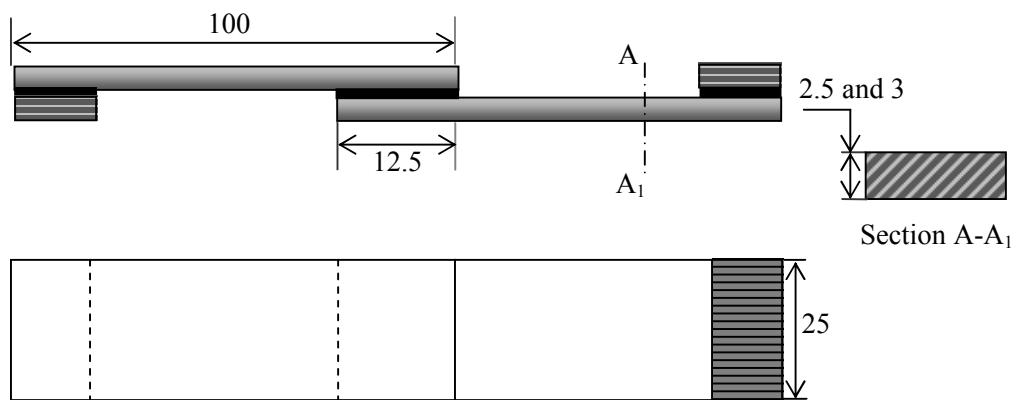


Fig.4. Single lap joint (dimensions in mm).

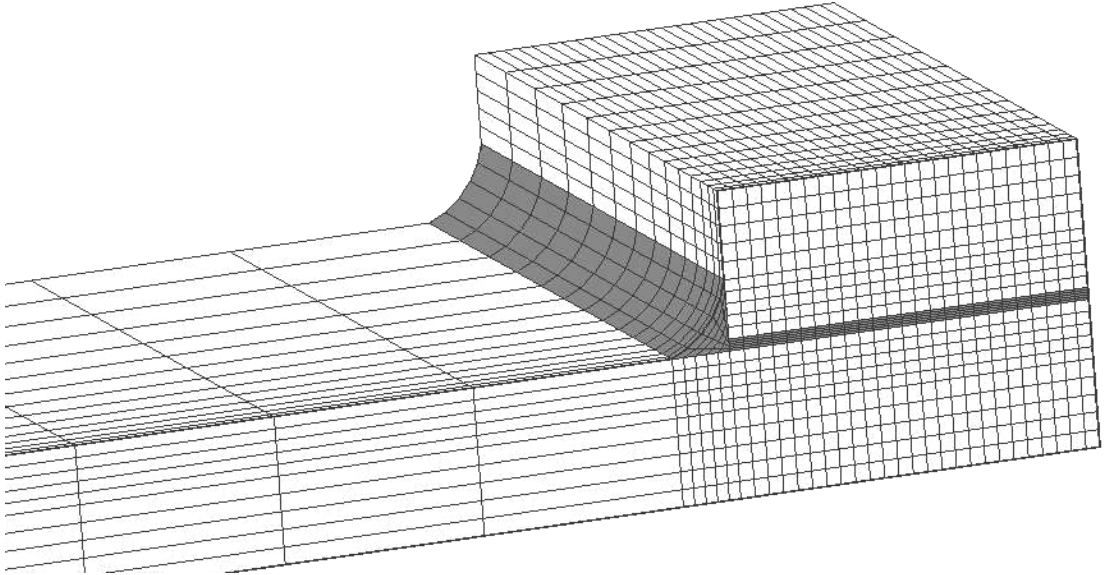


Fig. 5. Typical mesh used for 3D crack propagation.

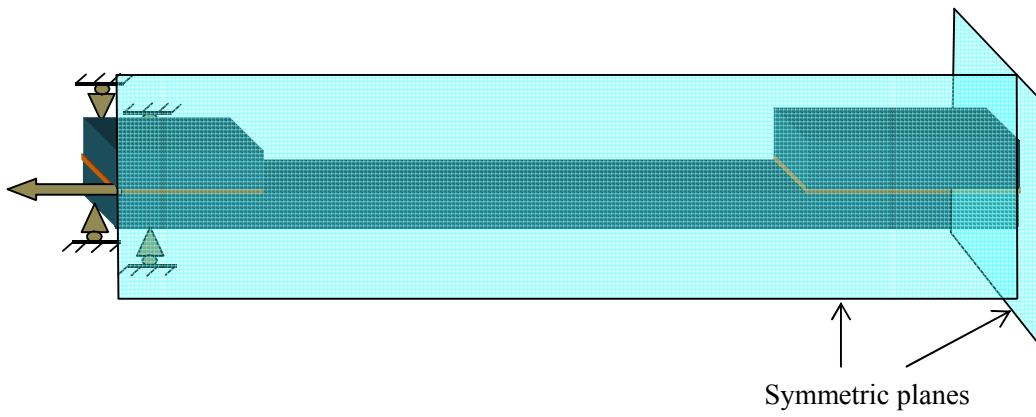


Fig. 6. Schematic sketch showing boundary conditions used for the analysis

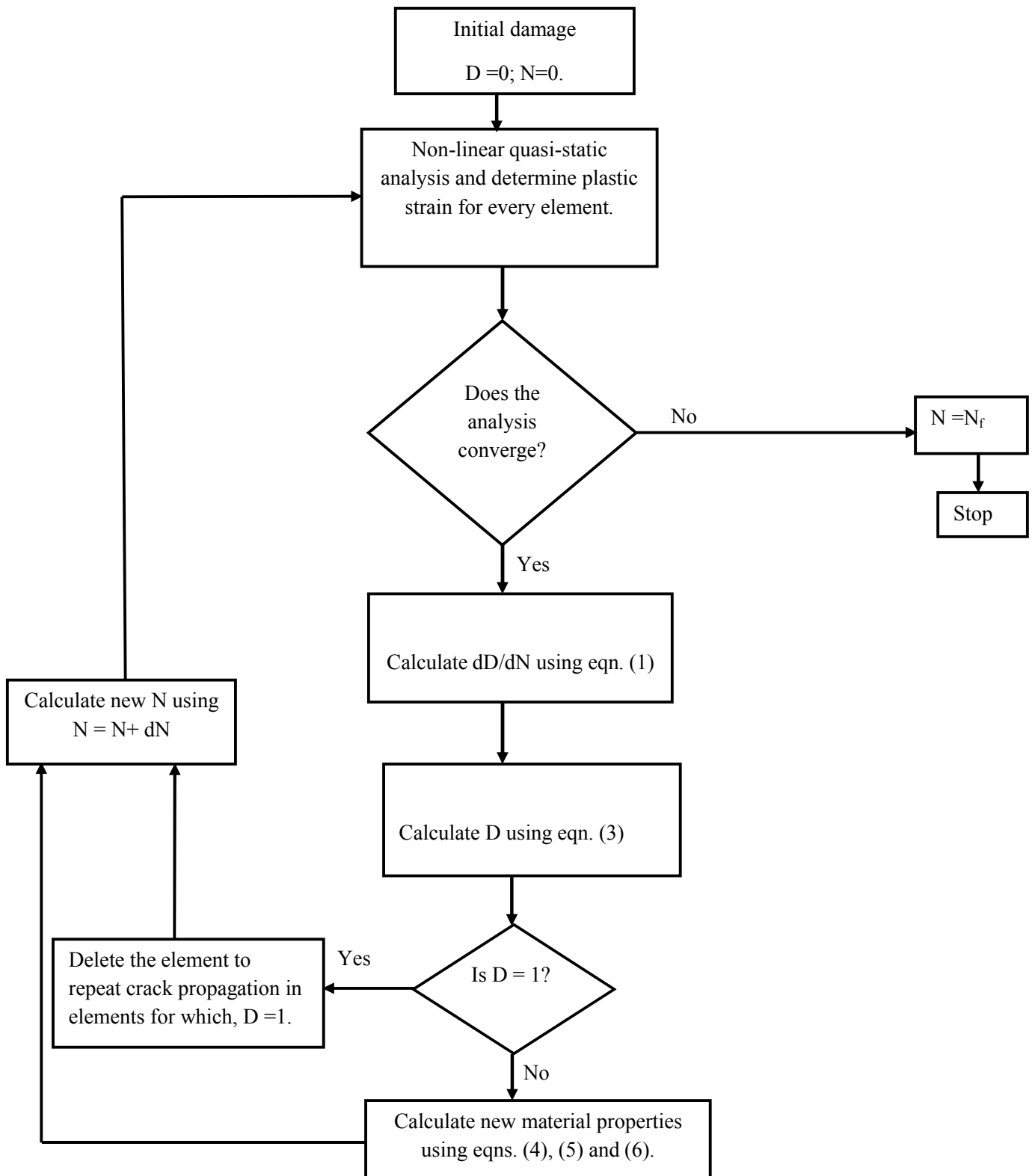
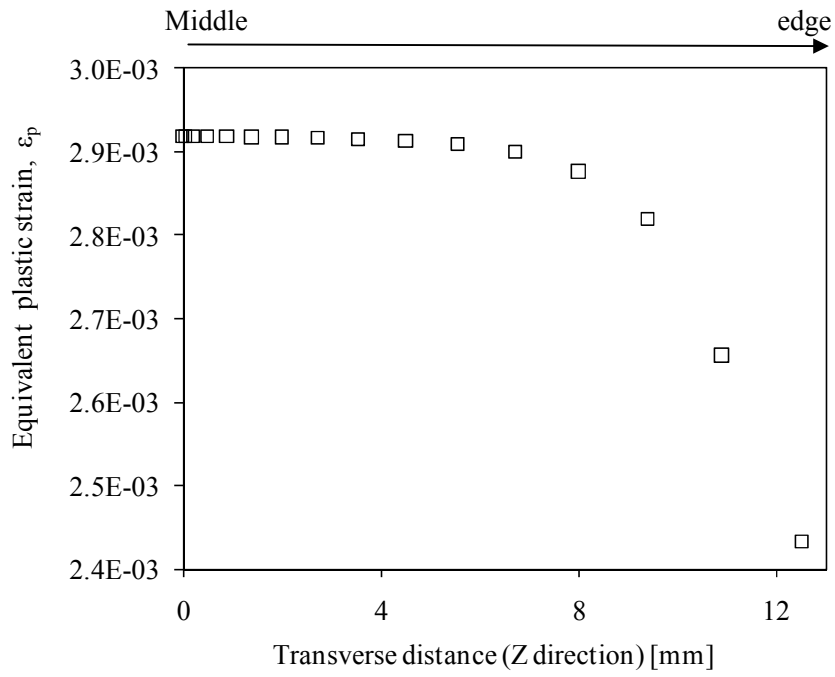
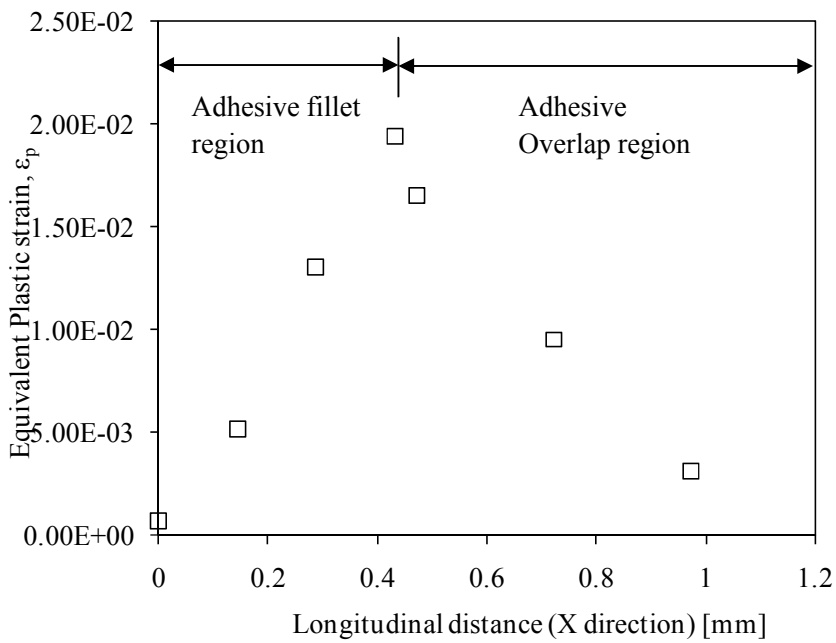


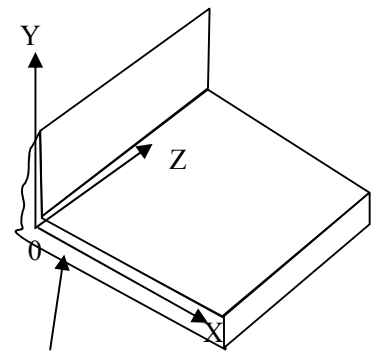
Fig. 7. Algorithm for DM based fatigue prediction.



(a)

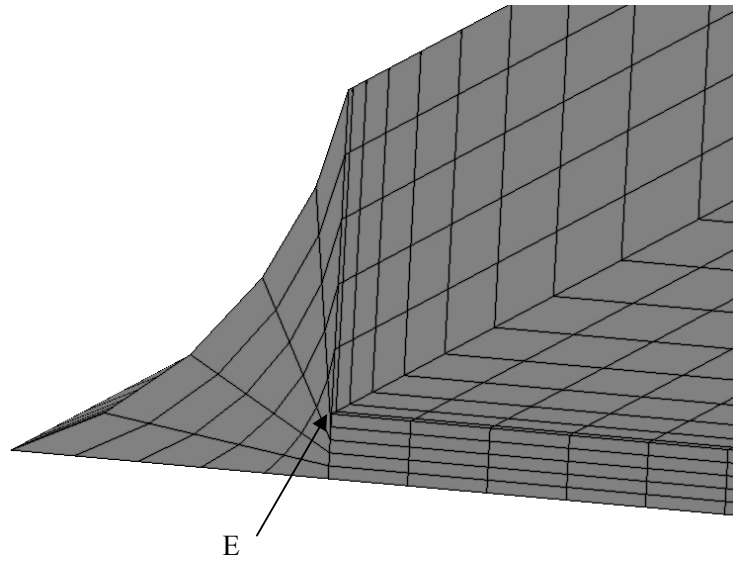


(b)

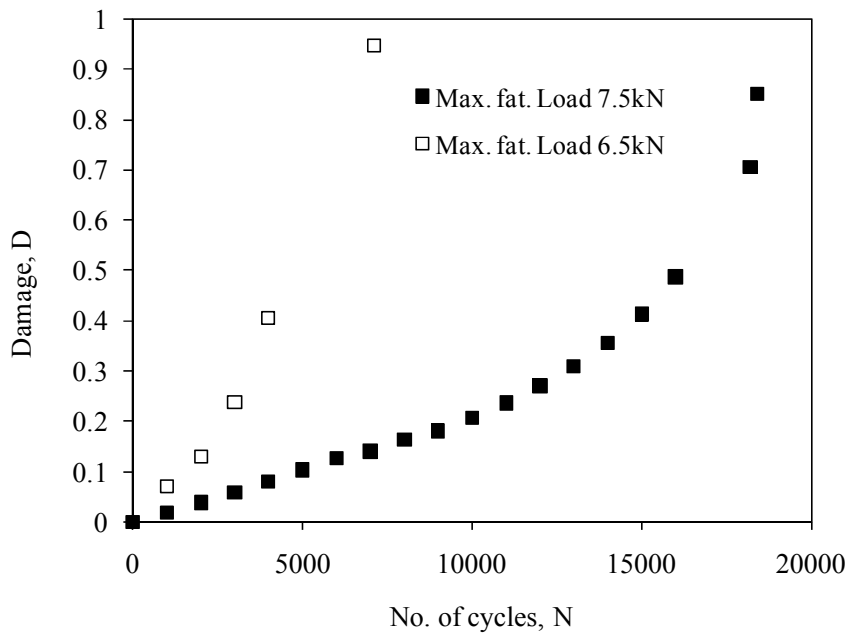


Plane of symmetry at  $Z = 0$   
(Middle of sample width)

Fig.8. Equivalent plastic strain distribution plotted (a) along the adhesive glue line and (b) across the width for the SLJ.



(a)



(b)

Fig.9. (a) Element E, in the embedded corner region, (b) Damage in element E prior to initial crack as a function of cycles for different fatigue loads.



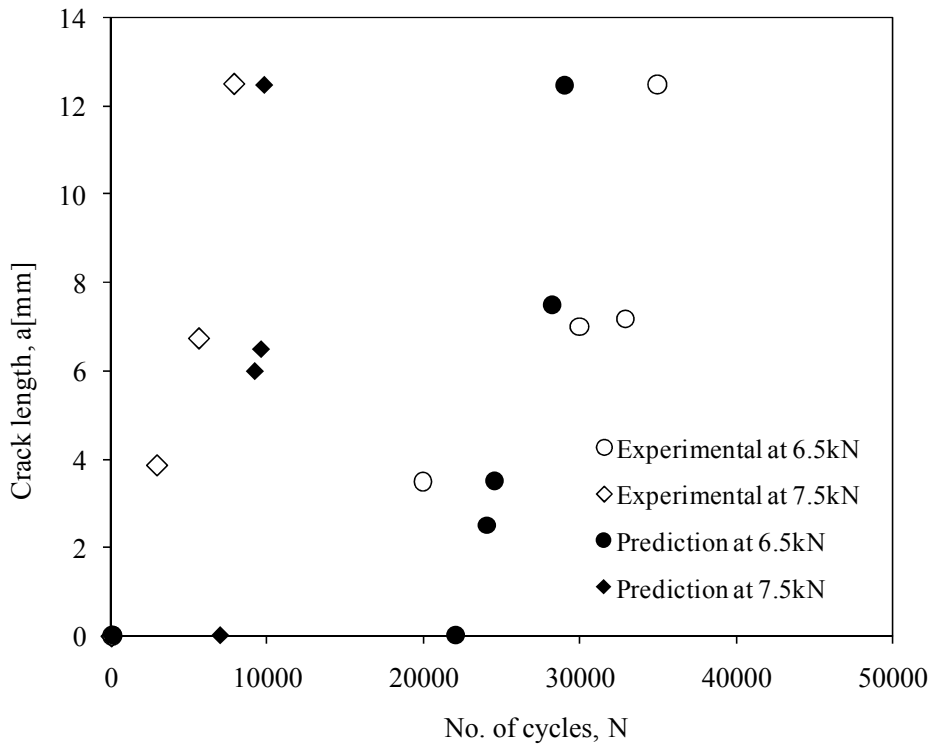
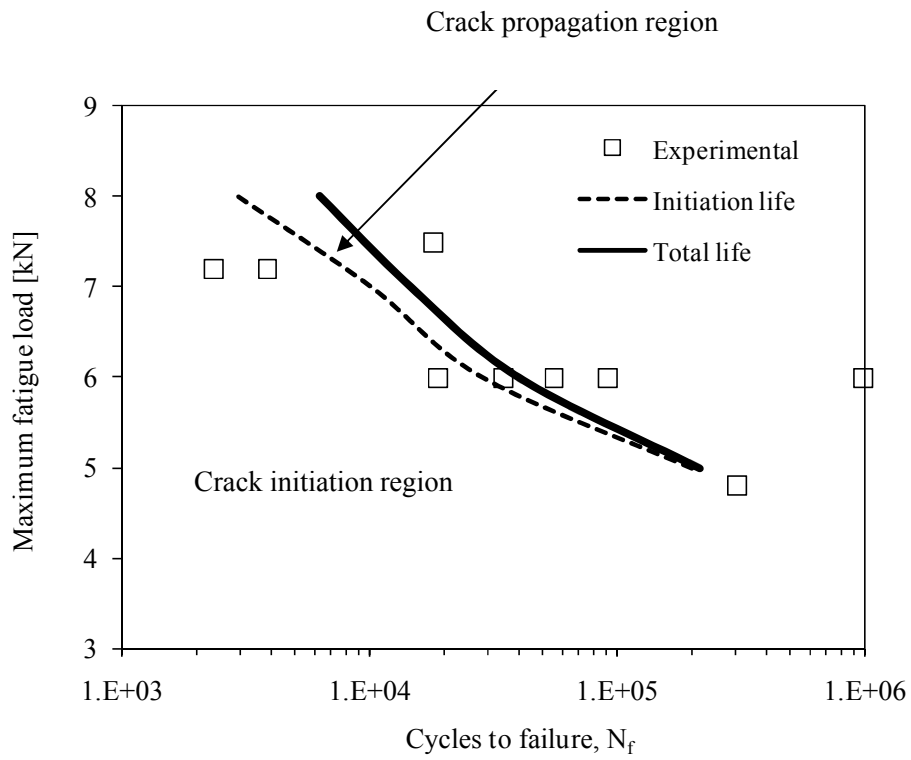
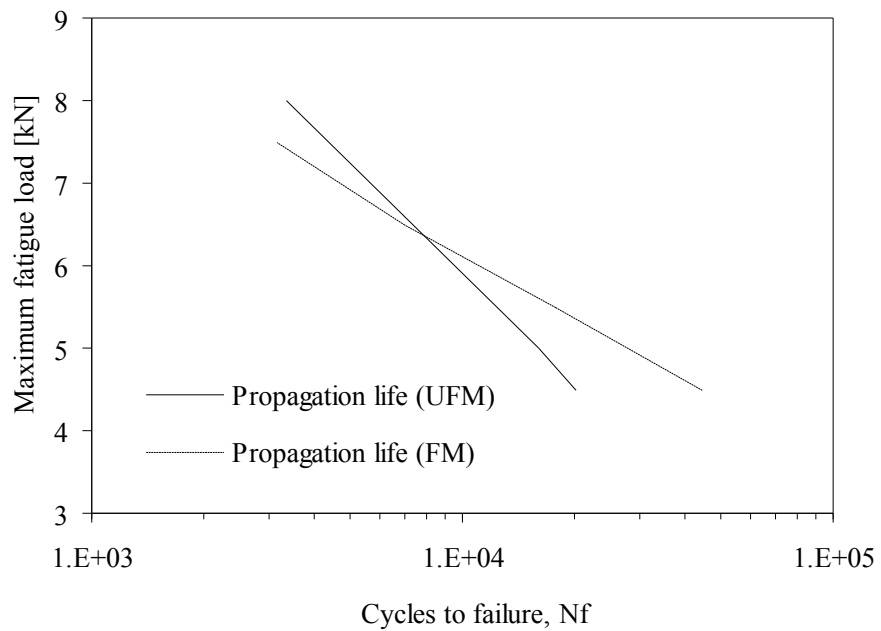


Fig.10. Comparison of crack growth prediction with experimental crack growth for different fatigue loads.



(a)



(b)

Fig.11. (a) extended L-N curve using UFM and (b) comparison between FM and UFM for propagation lives.

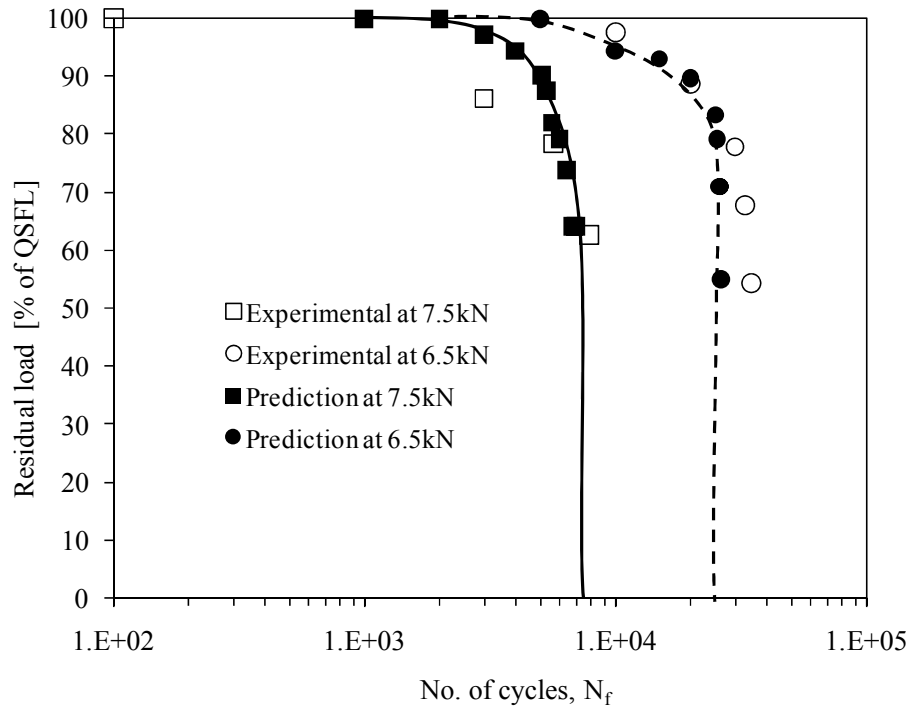


Fig. 12. Comparison between experimental and predicted strength wearout for different maximum fatigue loads.

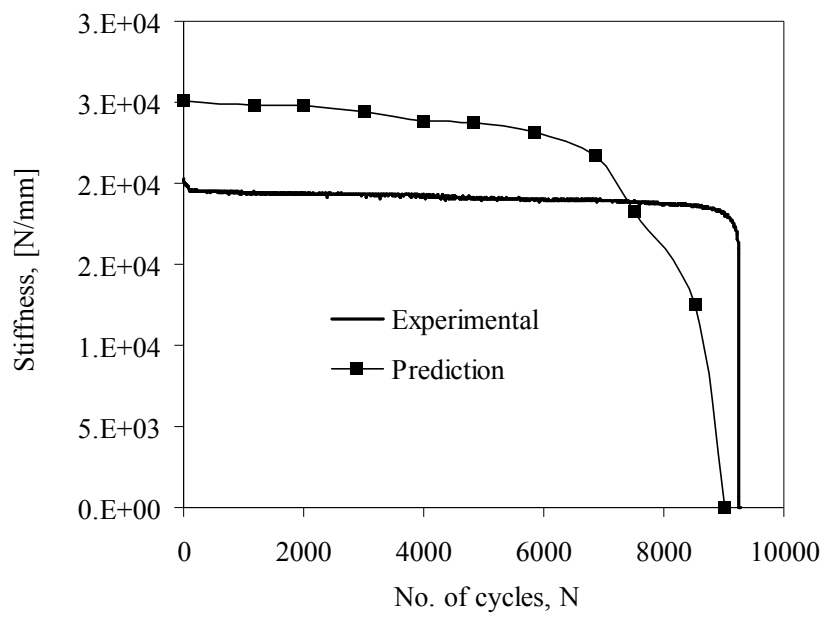


Fig. 13. Comparison between experimental and predicted stiffness wearout for maximum fatigue load equal to 7.5kN.

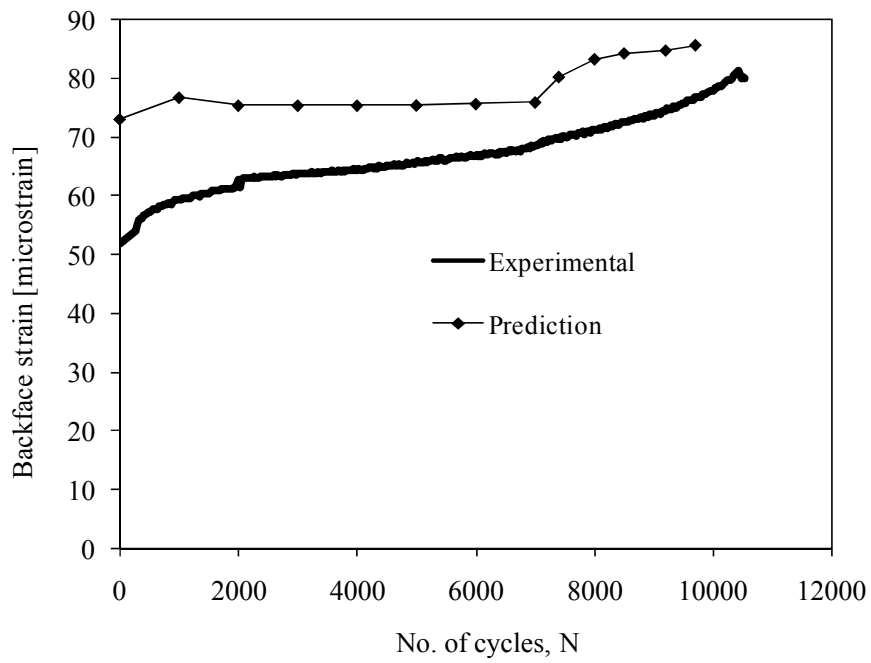


Fig. 14. Comparison between experimental and predicted BFS for maximum fatigue load equal to 7.5kN.

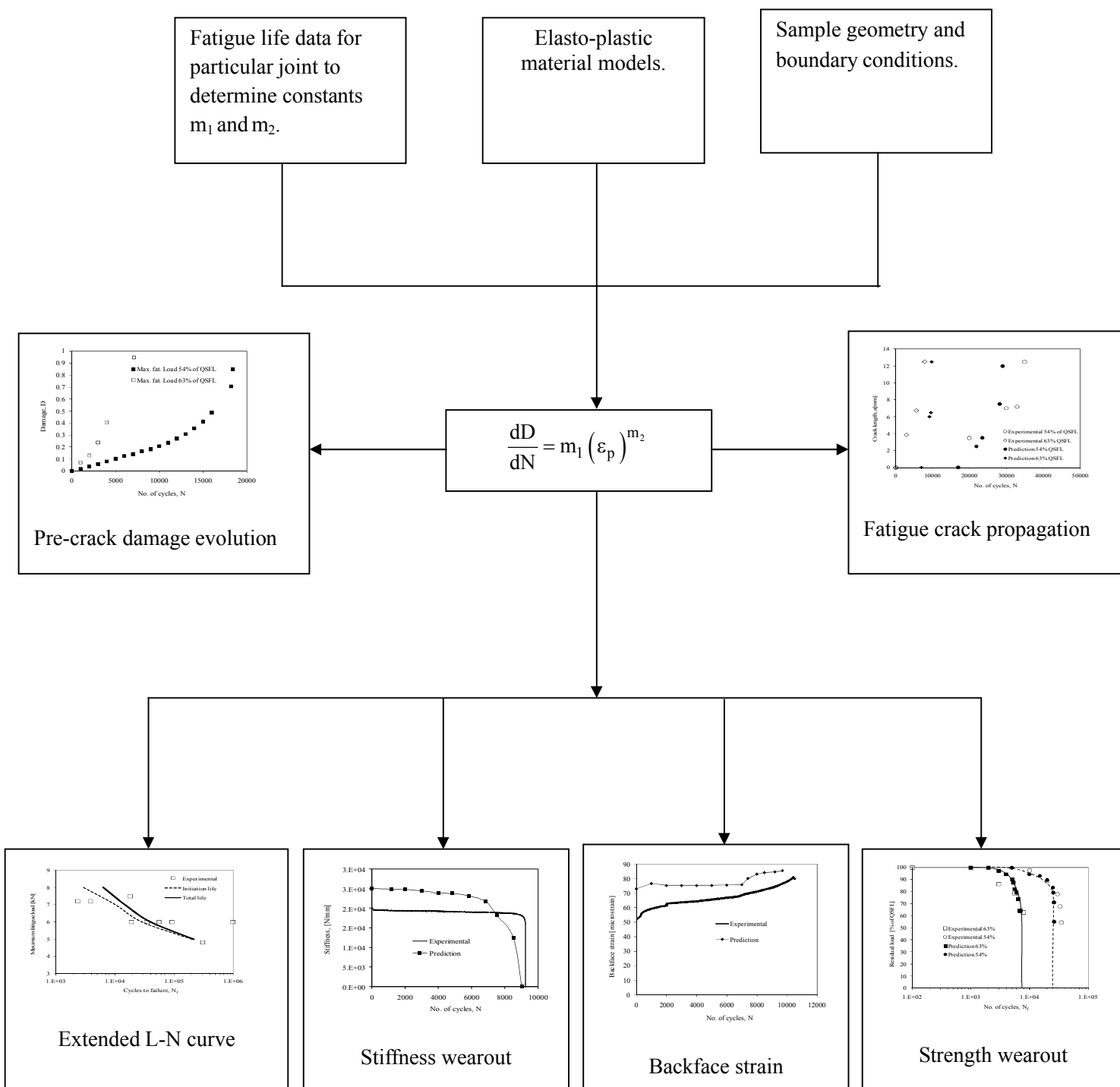


Fig. 15. UFM summarised with inputs and outputs for SLJ under constant amplitude fatigue loading.